应用数学和力学
APPLIED MATHEMATICS AND MECHANICS

双侧弹性约束悬臂梁的非光滑擦边动力学

史美娇，徐慧东，张建文

Non-Smooth Grazing Dynamics for Cantilever Beams With Bilateral Elastic Constraints

SHI Meijiao, XU Huidong, and ZHANG Jianwen

在线阅读 View online: https://doi.org/10.21656/1000-0887.420177

http://www.applmathmech.cn

双侧弹性约束悬臂梁的非光滑擦边动力学*

史美娇[1]，　徐慧东[2]，　张建文[1]

（1. 太原理工大学 数学学院，太原 030024；
2. 太原理工大学 机械与运载工程学院，太原 030024）

摘要：　研究了具有双侧弹性约束的单自由度悬臂梁系统擦边诱导的非光滑动力学行为. 首先, 基于弹性碰撞悬臂梁的动力学方程和擦边点的定义, 分析了双侧擦边周期运动的存在性条件. 其次, 选取零速度的 Poincaré截面, 推导了双侧擦边轨道附近带参数的高阶不连续映射. 然后, 结合光滑流映射和高阶不连续映射建立了新的复合分段范式映射. 最后, 将基于低阶范式映射和高阶范式映射得到的分岔图进行对比, 分析验证了高阶范式映射的有效性, 并通过数值仿真进一步揭示了弹性碰撞悬臂梁的擦边动力学.

关　键　词：　悬臂梁；　双侧弹性约束；　不连续映射；　擦边非光滑分岔

中图分类号：　O357.41　　**文献标志码：**　A　　DOI：10.21656/1000-0887.420177

Non-Smooth Grazing Dynamics for Cantilever Beams With Bilateral Elastic Constraints

SHI Meijiao[1]，　XU Huidong[2]，　ZHANG Jianwen[1]

（1. *College of Mathematics*, *Taiyuan University of Technology*, *Taiyuan* 030024, *P.R.China*;
2. *College of Mechanical and Vehicle Engineering*, *Taiyuan University of Technology*, *Taiyuan* 030024, *P.R.China*）

Abstract: The grazing-induced non-smooth dynamical behaviors of single-degree-of-freedom cantilever beam systems with bilateral elastic constraints were studied. Firstly, based on the dynamical equations for the cantilever beam under elastic impacts and the definition of grazing points, the existence condition for the bilateral grazing periodic motion was analyzed. Secondly, the zero-velocity Poincaré section was selected to derive the high-order discontinuous mapping with parameters near bilateral grazing orbits. Then a new composite piecewise normal form mapping was established through combination of the smooth flow mapping and the high-order discontinuous mapping. Finally, the validity of the high-order mapping was verified through comparison of the bifurcation diagram of the low-order mapping with that of the high-order mapping, and the grazing dynamics of the cantilever beam under elastic impacts were further revealed through numerical simulation.

Key words: cantilever beam; bilateral elastic constraint; discontinuous mapping; grazing non-smooth bifurcation

引　　言

梁作为工程中最常见的结构单元, 广泛应用于航空航天、汽车、海洋工程、机械工程等领域. 在应用设计

* **收稿日期：**　2021-06-28; **修订日期：**　2021-08-13
基金项目：　国家自然科学基金 (11872264)
作者简介：　史美娇 (1996—), 女, 硕士生 (E-mail: a2762440878@163.com);
张建文 (1962—), 男, 教授, 博士 (通讯作者. E-mail: zhangjianwen@tyut.edu.cn).
引用格式：　史美娇, 徐慧东, 张建文. 双侧弹性约束悬臂梁的非光滑擦边动力学[J]. 应用数学和力学, 2022, **43**(6): 619-630.

时经常需要考虑这类结构在碰撞冲击作用下的承载能力, 因此碰撞冲击作用下梁的动力学行为具有重要的研究价值.

反复持续碰撞的梁是一种典型的非光滑动力系统, 系统中碰撞的非光滑因素会使系统发生一种特殊的擦边现象, 即运动轨线以零速度与约束面接触. 定性研究擦边动力学的常用工具是不连续映射方法, 基于该方法得到的擦边规范形复合映射在一定程度上可以描述擦边点附近的动力学行为. Nordmark [1] 首先引入了不连续映射的概念, 为后续的许多研究奠定了基础. Chin 等[2] 基于不连续映射方法揭示了三种余维一的擦边分岔行为. Lamba 和 Budd [3] 调查了擦边分岔邻域内不连续映射的 Lyapunov 指数, 并揭示了最大 Lyapunov 指数在擦边邻域内的跳跃现象. Fredriksson 和 Nordmark [4] 推导了多自由度碰撞振动系统的局部零时间不连续映射的规范式, 并确立了擦边分岔的稳定性准则. Li 等[5] 和 Xu 等[6] 利用不连续映射方法研究了一般n自由度碰撞振动系统单擦边轨道和双擦边轨道附近的动力学行为, 并给出了双擦边轨道的稳定性条件. 以上文献都是基于低阶的擦边复合映射来调查擦边附近的动力学行为, 然而低阶的规范形映射在某些特殊参数范围内无法真实反应原系统的擦边动力学. 针对这个问题, Weger 等[7] 和 Molenaar 等[8] 修正了单自由度碰撞系统的低阶零时间不连续映射范式, 并调查了修正项对擦边分岔行为的影响. Zhao [9] 对一类单自由度刚性碰撞振子的 Poincaré不连续映射 (PDM) 的范式作了修正, 并通过数值仿真验证了范式的正确性. Yin 等[10] 推导获得了一般碰撞系统的高阶零时间不连续映射, 并基于高阶映射调查了擦边附近周期一运动的存在性, 通过与低阶映射比较, 验证了高阶不连续映射的有效性. 据笔者所知, 通过推导高阶的 PDM 分段映射来研究弹性碰撞系统的双擦边轨道附近的动力学行为尚未有报道.

本文以一类双侧弹性约束的单自由度悬臂梁为研究对象, 调查了双擦边周期运动的存在性, 推导了双擦边周期运动附近带参数的高阶 PDM 分段映射, 并结合光滑流映射获得了新的复合范式映射, 通过数值仿真对低阶映射和高阶映射反应的擦边分岔进行比较, 验证了高阶范式映射的有效性, 并揭示了双边弹性碰撞悬臂梁的擦边动力学.

1 系统模型及其动力学方程

图 1 为具有双侧弹性约束的悬臂梁系统, 系统的质量主要集中在悬臂梁的自由端, 用质量为 $\bar{m}$的圆形质块M来表示, 悬臂梁的长度为 l, 取 M 静平衡位置为坐标原点, 质块 M受到简谐激振力 $F=\bar{e}\bar{\omega}^2\sin(\bar{\omega}\bar{t})$的作用作竖直方向的运动. 上下约束分别由刚度为 $\bar{k}_1$和 $\bar{k}_2$的线性弹簧构成, 上下约束与质块 M静平衡位置存在的间隙都为 $\bar{d}$.

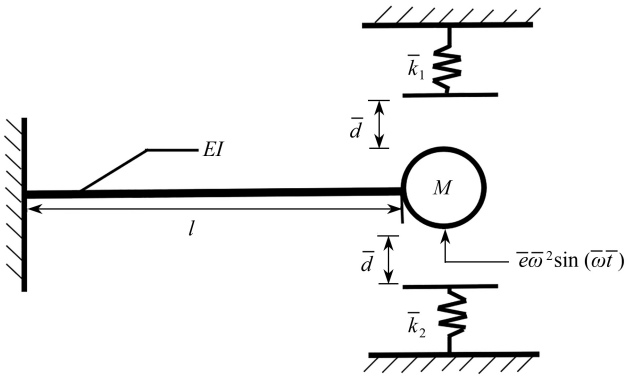

图 1 双侧弹性碰撞悬臂梁系统模型

Fig. 1 The cantilever beam system under bilateral elastic impacts

该系统满足如下的动力学方程 [11-12]:

$$\bar{m}\ddot{\bar{x}}+\bar{v}\bar{m}\dot{\bar{x}}+\bar{k}\bar{x}+\bar{K}(x)=\bar{e}\bar{\omega}^2\sin(\bar{\omega}\bar{t}), \tag{1}$$

这里 “$\cdot$” 表示对有量纲时间 $\bar{t}$求导数, $\bar{k}=3EI/\bar{l}^3$, 式中 E 为弹性模量, I 为悬臂梁的截面惯性矩. $\bar{K}(x)$ 具有如下的分段函数形式:

$$\overline{K}(x)=\begin{cases}\overline{k}_1(\overline{x}-\overline{d}), & \overline{x}>\overline{d},\\ 0, & -\overline{d}\leqslant\overline{x}\leqslant\overline{d},\\ \overline{k}_2(\overline{x}+\overline{d}), & \overline{x}<-\overline{d}.\end{cases}$$

引入无量纲量

$$x=\overline{x}\,\overline{m}/\overline{e},\ v=\overline{v}/\sqrt{\overline{k}/\overline{m}},\ w=\overline{\omega}/\sqrt{\overline{k}/\overline{m}},\ t=\sqrt{\overline{k}/\overline{m}}\cdot\overline{t},\ d=\overline{d}\,\overline{m}/\overline{e},\ k_i=\overline{k}_i/\overline{k}\qquad(i=1,2).$$

使用上面的无量纲量, 方程 (1)可转化为如下的无量纲形式:

$$\ddot{x}+v\dot{x}+x+K(x)=w^2\sin(wt),\tag{2}$$

其中

$$K(x)=\begin{cases}k_1(x-d), & x>d,\\ 0, & -d\leqslant x\leqslant d,\\ k_2(x+d), & x<-d.\end{cases}$$

2　擦边周期运动

这一节将根据擦边点的定义来给出双擦边周期运动的存在性条件. 为了描述擦边周期运动, 引入两个分界面, 首先定义边界函数

$$H_1(\boldsymbol{X},\mu)=x-d,\ H_2(\boldsymbol{X},\mu)=x+d,\tag{3}$$

其中 $\boldsymbol{X}=(x,\dot{x},\theta)^{\mathrm{T}}$, μ为间隙参数 d.

基于边界函数 (3), 定义如下分界面 1 和分界面 2:

$$\begin{aligned}\Sigma_1&=\{(x,\dot{x},\theta)^{\mathrm{T}}\in R^3|H_1(\boldsymbol{X},\mu)=0\},\\ \Sigma_2&=\{(x,\dot{x},\theta)^{\mathrm{T}}\in R^3|H_2(\boldsymbol{X},\mu)=0\},\end{aligned}\tag{4}$$

这里, Σ_1表示质块 M 与上约束刚接触或刚分离, Σ_2 表示质块 M 与下约束刚接触或刚分离, 其中 $\theta=\omega t+\tau$.

两个分界面 Σ_1和 Σ_2可将系统的状态空间分成三部分, 如图 2 所示. 图 2 中的区域 V_{c}, V_{u}, V_{d}具有如下的意义:

区域 $V_{\mathrm{u}}=\{(x,\dot{x},\theta)^{\mathrm{T}}\in R^3|H_1(\boldsymbol{X},\mu)\geqslant 0\}$表示物块与上约束保持接触状态;

区域 $V_{\mathrm{d}}=\{(x,\dot{x},\theta)^{\mathrm{T}}\in R^3|H_2(\boldsymbol{X},\mu)\leqslant 0\}$表示物块与下约束保持接触状态;

区域 $V_{\mathrm{c}}=\{(x,\dot{x},\theta)^{\mathrm{T}}\in R^3|(x,\dot{x},\theta)^{\mathrm{T}}\in\overline{V}_{\mathrm{u}}\cap\overline{V}_{\mathrm{d}}\}$表示物块与上下约束都不接触.

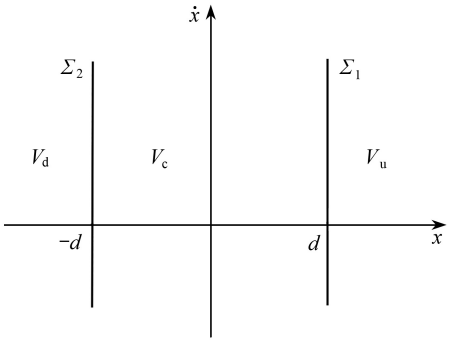

图 2　弹性碰撞悬臂梁系统 (2) 的二维相平面

Fig. 2　The 2D phase plane of the cantilever beam system under bilateral elastic impacts (2)

基于上面的区域, 且考虑 $k_1=k_2=k$, 将系统 (2) 转化成如下的自治系统:

$$\dot{\boldsymbol{X}}=\boldsymbol{F}(\boldsymbol{X},\mu)=\begin{cases}\boldsymbol{F}_1(\boldsymbol{X},\mu), & \boldsymbol{X}\in V_{\mathrm{c}},\\ \boldsymbol{F}_2(\boldsymbol{X},\mu), & \boldsymbol{X}\in V_{\mathrm{u}},\\ \boldsymbol{F}_3(\boldsymbol{X},\mu), & \boldsymbol{X}\in V_{\mathrm{d}},\end{cases}\tag{5}$$

其中

$$\boldsymbol{F}_1(\boldsymbol{X},\mu)=\begin{pmatrix}\dot{x}\\ w^2\sin(wt)-x-v\dot{x}\end{pmatrix},\ \boldsymbol{F}_2(\boldsymbol{X},\mu)=\begin{pmatrix}\dot{x}\\ w^2\sin(wt)-x-v\dot{x}-k(x-d)\end{pmatrix},$$

$$\boldsymbol{F}_3(\boldsymbol{X},\mu)=\begin{pmatrix}\dot{x}\\ w^2\sin(wt)-x-v\dot{x}-k(x+d)\end{pmatrix}.$$

系统 (5)在区间 $V_{\rm c},V_{\rm u},V_{\rm d}$内的通解分别为

$$\boldsymbol{X}_{\rm c}=\begin{pmatrix}\mathrm{e}^{-vt/2}(a_1\cos(u_1t)+b_1\sin(u_1t))+A_1\sin(wt+\tau)+B_1\cos(wt+\tau)\\ \mathrm{e}^{-vt/2}\left(\left(b_1u_1-\dfrac{v}{2}a_1\right)\cos(u_1t)-\left(a_1u_1+\dfrac{v}{2}b_1\right)\sin(u_1t)\right)+A_1w\cos(wt+\tau)-B_1w\sin(wt+\tau)\\ wt+\tau\end{pmatrix},\tag{6}$$

$$\boldsymbol{X}_{\rm u}=\begin{pmatrix}\mathrm{e}^{-vt/2}(a_2\cos(u_2t)+b_2\sin(u_2t))+A_2\sin(wt+\tau)+B_2\cos(wt+\tau)+kd/(1+k)\\ \mathrm{e}^{-vt/2}\left(\left(b_2u_2-\dfrac{v}{2}a_2\right)\cos(u_2t)-\left(a_2u_2+\dfrac{v}{2}b_2\right)\sin(u_2t)\right)+A_2w\cos(wt+\tau)-B_2w\sin(wt+\tau)\\ wt+\tau\end{pmatrix},\tag{7}$$

$$\boldsymbol{X}_{\rm d}=\begin{pmatrix}\mathrm{e}^{-vt/2}(a_3\cos(u_3t)+b_3\sin(u_3t))+A_3\sin(wt+\tau)+B_3\cos(wt+\tau)-kd/(1+k)\\ \mathrm{e}^{-vt/2}\left(\left(b_3u_3-\dfrac{v}{2}a_3\right)\cos(u_3t)-\left(a_3u_3+\dfrac{v}{2}b_3\right)\sin(u_3t)\right)+A_3w\cos(wt+\tau)-B_3w\sin(wt+\tau)\\ wt+\tau\end{pmatrix},\tag{8}$$

其中, a_i和 $b_i(i=1,2,3)$为积分常数, $u_1=\sqrt{1-v^2/4}, u_2=u_3=\sqrt{1+k-v^2/4}$, A_i和 $B_i(i=1,2,3)$为振幅常数且具有如下形式:

$$\begin{cases}A_1=\dfrac{(1-w^2)w^2}{(1-w^2)^2+v^2w^2},\ B_1=\dfrac{-vw^3}{(1-w^2)^2+v^2w^2},\\ A_2=A_3=\dfrac{(1+k-w^2)w^2}{(1+k-w^2)^2+v^2w^2},\ B_2=B_3=\dfrac{-vw^3}{(1+k-w^2)^2+v^2w^2}.\end{cases}\tag{9}$$

擦边周期运动的周期条件为

$$x(0)=x\left(\frac{2\pi}{w}\right),\ \dot{x}(0)=\dot{x}\left(\frac{2\pi}{w}\right).\tag{10}$$

将系统 (5)在区间 $V_{\rm c}$内的通解 (6)代入式 (10) 中可得

$$\begin{pmatrix}1-\mathrm{e}^Tc_T & -\mathrm{e}^Ts_T\\ 0 & (1-\mathrm{e}^Tc_T)\left(u_1-u_1\mathrm{e}^Tc_T+\dfrac{v\mathrm{e}^Ts_T}{2}\right)+\mathrm{e}^Ts_T\left(\dfrac{v\mathrm{e}^Tc_T}{2}+u_1\mathrm{e}^Ts_T-\dfrac{v}{2}\right)\end{pmatrix}\begin{pmatrix}a_1\\ b_1\end{pmatrix}=\begin{pmatrix}0\\ 0\end{pmatrix},\tag{11}$$

其中 $\mathrm{e}^T=\exp\left(-\dfrac{v}{2}\dfrac{2\pi}{w}\right),\ c_T=\cos\left(u_1\dfrac{2\pi}{w}\right),\ s_T=\sin\left(u_1\dfrac{2\pi}{w}\right)$.

只考虑方程 (11)有唯一解的情况, 因此有

$$\begin{vmatrix}1-\mathrm{e}^Tc_T & -\mathrm{e}^Ts_T\\ 0 & (1-\mathrm{e}^Tc_T)\left(u_1-u_1\mathrm{e}^Tc_T+\dfrac{v\mathrm{e}^Ts_T}{2}\right)+\mathrm{e}^Ts_T\left(\dfrac{v\mathrm{e}^Tc_T}{2}+u_1\mathrm{e}^Ts_T-\dfrac{v}{2}\right)\end{vmatrix}\neq 0,\tag{12}$$

即满足

$$2\mathrm{e}^Tc_T-\mathrm{e}^{2T}-1\neq 0.\tag{13}$$

由不等式 (12)可知 $a_1=b_1=0$, 将其代入通解 (6)得到区域 $V_{\rm c}$内的特解为

$$x_t=A_1\sin(wt+\tau)+B_1\cos(wt+\tau).\tag{14}$$

以特解 (14) 来确定擦边分岔点, 设 $\boldsymbol{\Phi}_i(\boldsymbol{X},\mu,\delta), i=1,2,3$分别为系统相应向量场 $\boldsymbol{F}_i(\boldsymbol{X},\boldsymbol{\mu})$ 的流函数, 且满足

$$\frac{\partial\boldsymbol{\Phi}_i(\boldsymbol{X},\mu,\delta)}{\partial t}=\boldsymbol{F}_i(\boldsymbol{\Phi}_i(\boldsymbol{X},\mu,\delta)),\ \boldsymbol{\Phi}_i(\boldsymbol{X},\mu,0)=\boldsymbol{X},$$

以及周期轨道与分界面 Σ_1的擦切点为 $\boldsymbol{X}_1^*$. 根据擦边轨道的定义需要满足下面的条件:

$$\begin{cases}H_1(\boldsymbol{X}_1^*,\mu^*)=A_1\sin\tau+B_1\cos\tau-d=0,\\ v_{1\rm c}^*=\dfrac{\partial H_1(\boldsymbol{\Phi}_1(\boldsymbol{X}_1^*,\mu^*,0),\mu^*)}{\partial\delta}=H_{1,\boldsymbol{X}}\boldsymbol{F}_{1s}(\boldsymbol{X}_1^*,\mu^*)=A_1w\cos\tau-B_1w\sin\tau=0,\\ a_{1\rm c}^*=\dfrac{\partial^2H_1(\boldsymbol{\Phi}_1(\boldsymbol{X}_1^*,\mu^*,0),\mu^*)}{\partial\delta^2}=v_{1\rm c,\boldsymbol{X}}^*\boldsymbol{F}_{1s}^*=w^2\sin\tau-d<0,\end{cases}\tag{15}$$

这里, $v_{1\rm c}^*$表示 $V_{\rm c}$区域内的擦边轨道与上约束面 Σ_1的擦切速度, $\boldsymbol{F}_{1s}^*$表示 $V_{\rm c}$区域内的向量场在 $\boldsymbol{X}_1^*$处的值, $a_{1\rm c}^*$表示 $V_{\rm c}$区域内擦切点 $\boldsymbol{X}_1^*$处的加速度. 由式 (15)的前两个等式可得到临界擦边分岔参数满足的关系式为

$$G(\mu^*)=d^{*2}-\frac{(1-w^{*2})^2w^{*4}+v^{*2}w^{*6}}{((1-w^{*2})^2+v^{*2}w^{*2})^2}=0, \tag{16}$$

这里“μ^*”可以是 d^*, w^*和 v^*中的任意一个参数, 相应可求得 $\tau=\arctan(A_1/B_1)$.

当双擦周期运动轨线刚好到达下约束面时, 设周期轨道与下约束面 Σ_2 的擦切点为 $\boldsymbol{X}_2^*$, 根据擦边轨道的定义有

$$\begin{cases} H_2(\boldsymbol{X}_2^*,\mu^*)=A_1\sin\tau+B_1\cos\tau+d=0,\\ v_{2c}^*=\dfrac{\partial H_2(\boldsymbol{\Phi}_1(\boldsymbol{X}_2^*,\mu^*,0),\mu^*)}{\partial\delta}=H_{2,\boldsymbol{X}}\boldsymbol{F}_{1x}(\boldsymbol{X}_2^*,\mu^*)=A_1w\cos\tau-B_1w\sin\tau=0,\\ a_{2c}^*=\dfrac{\partial^2 H_2(\boldsymbol{\Phi}_1(\boldsymbol{X}_2^*,\mu^*,0),\mu^*)}{\partial\delta^2}=v_{2c,\boldsymbol{X}}^*\boldsymbol{F}_{1x}^*=w^2\sin\tau+d>0. \end{cases} \tag{17}$$

根据下约束的擦边分岔条件 (17)可得到和方程 (16)同样的擦边临界参数关系式以及同样的相位角 $\tau=\arctan(A_1/B_1)$.

命题 1　当弹性碰撞悬臂梁系统 (2) 满足下面的条件:

① 周期条件: $2\mathrm{e}^{T}c_T-\mathrm{e}^{2T}-1\neq 0$;

② 擦边条件: $d^*=\sqrt{\dfrac{(1-w^{*2})^2w^{*4}+v^{*2}w^{*6}}{((1-w^{*2})^2+v^{*2}w^{*2})^2}}$, $\tau^*=\arctan(A_1/B_1)$;

③ 非黏附条件: $|\sin\tau^*|<\dfrac{d^*}{w^{*2}}$,

系统存在周期为 $T=\dfrac{2\pi}{w}$的双擦边周期轨道.

3　Poincaré不连续映射及复合映射

本节选取速度为零的 Poincaré 截面来推导弹性约束悬臂梁系统 (2)双擦边周期运动的不连续映射. 定义两个零速度的 Poincaré 截面:

$$\Pi_1=\{\boldsymbol{X}_1\in D_1|v_1(\boldsymbol{X}_1,\mu)=0\},\ \Pi_2=\{\boldsymbol{X}_2\in D_2|v_2(\boldsymbol{X}_2,\mu)=0\}, \tag{18}$$

这里 D_1是上方约束截面 Σ_1的擦边点 $\boldsymbol{X}_1^*$ 附近的区域, D_2是下方约束截面 Σ_2的擦边点 $\boldsymbol{X}_2^*$ 附近的区域.

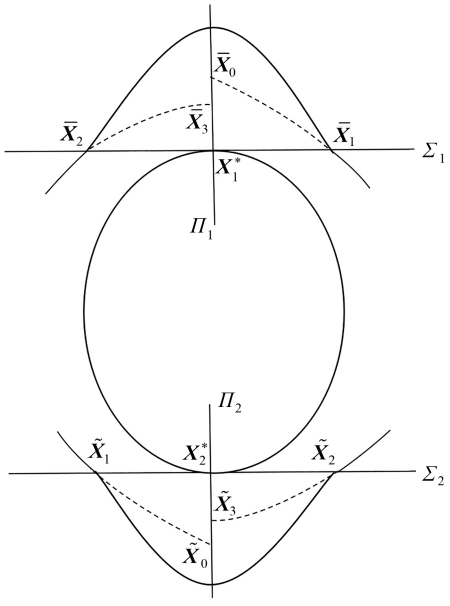

图 3　擦边点附近不连续映射 $\boldsymbol{P}_{\mathrm{PDM1}}$和 $\boldsymbol{P}_{\mathrm{PDM2}}$的示意图

Fig. 3　The schematic diagram of the discontinuity mappings $\boldsymbol{P}_{\mathrm{PDM1}}$ and $\boldsymbol{P}_{\mathrm{PDM2}}$ near grazing points

下面来构造擦边点 $\boldsymbol{X}_1^*$附近的不连续映射 $\boldsymbol{P}_{\mathrm{PDM1}}$ 和擦边点 $\boldsymbol{X}_2^*$附近的不连续映射 $\boldsymbol{P}_{\mathrm{PDM2}}$. 首先构造 $\boldsymbol{P}_{\mathrm{PDM1}}$, 从擦边点 $\boldsymbol{X}_1^*$的邻域内位于零速度截面 Π_1上一点 $\overline{\boldsymbol{X}}_0$出发, 由流函数 $\boldsymbol{\Phi}_1$ 经过时间 δ_1到达碰撞面 Σ_1 上的点 $\overline{\boldsymbol{X}}_1$, 其中 $\delta_1<0$. 再由流函数 $\boldsymbol{\Phi}_2$经过时间 δ_2 到达碰撞面上 Σ_1的点 $\overline{\boldsymbol{X}}_2$, 最后由流函数 $\boldsymbol{\Phi}_1$经过时间 $-\delta_3$ 到达零速度截面

Π_1上的点 $\overline{\boldsymbol{X}}_3$. 即 $\boldsymbol{P}_{\mathrm{PDM1}}(\overline{\boldsymbol{X}}_0,\mu)=\boldsymbol{\Phi}_1(\boldsymbol{\Phi}_2(\boldsymbol{\Phi}_1(\overline{X}_0,\mu,\delta_1),\mu,\delta_2),\mu,\delta_3)$; $\boldsymbol{P}_{\mathrm{PDM2}}$ 的构造和 $\boldsymbol{P}_{\mathrm{PDM1}}$类似, 于是有 $\boldsymbol{P}_{\mathrm{PDM2}}(\tilde{\boldsymbol{X}}_0,\mu)=\boldsymbol{\Phi}_1(\boldsymbol{\Phi}_3(\boldsymbol{\Phi}_1(\tilde{\boldsymbol{X}}_0,\mu,t_1),\mu,t_2),\mu,t_3)$, 如图 3 所示.

3.1 低阶复合范式映射

首先来详细推导不连续映射 $\boldsymbol{P}_{\mathrm{PDM1}}$ 的表达式, 低阶范式映射中时间符号记为 $\bar{\delta}_i$和 $\bar{t}_i(i=1,2,3)$.

第一步, 从 $\overline{\boldsymbol{X}}_0$到 $\overline{\boldsymbol{X}}_1$, 计算所用的时间 $\bar{\delta}_1$.

将流函数 $\boldsymbol{\Phi}_1(\overline{\boldsymbol{X}}_0,\mu,\bar{\delta}_1)$在 $\overline{\boldsymbol{X}}_0=\boldsymbol{X}_1^*,\mu=\mu^*$和 $\bar{\delta}_1=0$ 处一阶 Taylor 展开有

$$\boldsymbol{X}_1=\boldsymbol{\Phi}_1(\overline{\boldsymbol{X}}_0,\mu,\bar{\delta}_1)=\overline{\boldsymbol{X}}_0+\boldsymbol{F}_{1s}^*\bar{\delta}_1+h.o.t., \tag{19}$$

*h.o.t.*表示被省略的高阶项.

因为 $\overline{\boldsymbol{X}}_1$ 在分界面 Σ_1上, 存在 $H_1(\overline{\boldsymbol{X}}_1,\mu)=0$. 将 $H_1(\overline{\boldsymbol{X}}_1,\mu)$ Taylor 展开, 并利用 $H_1(\overline{\boldsymbol{X}}_1,\mu)=0$有

$$\begin{aligned}
&H_1(\overline{\boldsymbol{X}}_1,\mu)=H_1(\boldsymbol{\Phi}_1(\overline{\boldsymbol{X}}_0,\mu,\bar{\delta}_1),\mu)=G_1(\overline{\boldsymbol{X}}_0,\mu,\bar{\delta}_1)=\\
&\quad G_1(\boldsymbol{X}_1^*,\mu^*,0)+G_{1,\overline{\boldsymbol{X}}_0}\big|_{\overline{\boldsymbol{X}}_0=\boldsymbol{X}_1^*,\mu=\mu^*,\bar{\delta}_1=0}(\overline{\boldsymbol{X}}_0-\boldsymbol{X}_1^*)+G_{1,\mu}\big|_{\overline{\boldsymbol{X}}_0=\boldsymbol{X}_1^*,\mu=\mu^*,\bar{\delta}_1=0}(\mu-\mu^*)+\\
&\quad G_{1,\bar{\delta}_1}\big|_{\overline{\boldsymbol{X}}_0=\boldsymbol{X}_1^*,\mu=\mu^*,\bar{\delta}_1=0}\bar{\delta}_1+G_{1,\overline{\boldsymbol{X}}_0,\bar{\delta}_1}\big|_{\overline{\boldsymbol{X}}_0=\boldsymbol{X}_1^*,\mu=\mu^*,\bar{\delta}_1=0}(\overline{\boldsymbol{X}}_0-\boldsymbol{X}_1^*)\bar{\delta}_1+\\
&\quad G_{1,\mu,\bar{\delta}_1}\big|_{\overline{\boldsymbol{X}}_0=\boldsymbol{X}_1^*,\mu=\mu^*,\bar{\delta}_1=0}(\mu-\mu^*)\bar{\delta}_1+G_{1,\overline{\boldsymbol{X}}_0,\overline{\boldsymbol{X}}_0}\big|_{\overline{\boldsymbol{X}}_0=\boldsymbol{X}_1^*,\mu=\mu^*,\bar{\delta}_1=0}(\overline{\boldsymbol{X}}_0-\boldsymbol{X}_1^*)^2+\\
&\quad G_{1,\mu,\mu}\big|_{\overline{\boldsymbol{X}}_0=\boldsymbol{X}_1^*,\mu=\mu^*,\bar{\delta}_1=0}(\mu-\mu^*)^2+\frac{1}{2}G_{1,\bar{\delta}_1,\bar{\delta}_1}\big|_{\overline{\boldsymbol{X}}_0=\boldsymbol{X}_1^*,\mu=\mu^*,\bar{\delta}_1=0}\bar{\delta}_1^2+h.o.t.=0,
\end{aligned} \tag{20}$$

式中

$$\begin{aligned}
&G_1(\boldsymbol{X}_1^*,\mu^*,0)=H_1(\boldsymbol{X}_1^*,\mu^*),\ G_{1,\overline{\boldsymbol{X}}_0}\big|_{\overline{\boldsymbol{X}}_0=\boldsymbol{X}_1^*,\mu=\mu^*,\bar{\delta}_1=0}=H_{1,\boldsymbol{X}}\boldsymbol{\Phi}_{1,\overline{\boldsymbol{X}}_0},\\
&G_{1,\mu}\big|_{\overline{\boldsymbol{X}}_0=\boldsymbol{X}_1^*,\mu=\mu^*,\bar{\delta}_1=0}=H_{1,\mu}(\boldsymbol{\Phi}_{1,\mu}+\boldsymbol{I}),\ G_{1,\bar{\delta}_1}\big|_{\overline{\boldsymbol{X}}_0=\boldsymbol{X}_1^*,\mu=\mu^*,\bar{\delta}_1=0}=H_{1,\boldsymbol{X}}\boldsymbol{F}_{1s}^*=v_{1\mathrm{c}},\\
&G_{1,\overline{\boldsymbol{X}}_0,\bar{\delta}_1}\big|_{\overline{\boldsymbol{X}}_0=\boldsymbol{X}_1^*,\mu=\mu^*,\bar{\delta}_1=0}=\frac{\partial v_{1\mathrm{c}}}{\partial\boldsymbol{X}}\Big|_{\overline{\boldsymbol{X}}_0=\boldsymbol{X}_1^*,\mu=\mu^*}=v_{1\mathrm{c},\boldsymbol{X}},\ G_{1,\mu,\bar{\delta}_1}\big|_{\overline{\boldsymbol{X}}_0=\boldsymbol{X}_1^*,\mu=\mu^*,\bar{\delta}_1=0}=\frac{\partial v_{1\mathrm{c}}}{\partial\mu}\Big|_{\overline{\boldsymbol{X}}_0=\boldsymbol{X}_1^*,\mu=\mu^*}=v_{1\mathrm{c},\mu},\\
&G_{1,\overline{\boldsymbol{X}}_0,\overline{\boldsymbol{X}}_0}\big|_{\overline{\boldsymbol{X}}_0=\boldsymbol{X}_1^*,\mu=\mu^*,\bar{\delta}_1=0}=\frac{\partial H_{1,\boldsymbol{X}}\boldsymbol{\Phi}_{1,\overline{\boldsymbol{X}}_0}}{\partial\overline{\boldsymbol{X}}_0}\Big|_{\overline{\boldsymbol{X}}_0=\boldsymbol{X}_1^*,\mu=\mu^*},\ G_{1,\mu,\mu}\big|_{\overline{\boldsymbol{X}}_0=\boldsymbol{X}_1^*,\mu=\mu^*,\bar{\delta}_1=0}=\frac{\partial H_{1,\mu}(\boldsymbol{\Phi}_{1,\mu}+\boldsymbol{I})}{\partial\mu}\Big|_{\overline{\boldsymbol{X}}_0=\boldsymbol{X}_1^*,\mu=\mu^*},\\
&G_{1,\bar{\delta}_1,\bar{\delta}_1}\big|_{\overline{\boldsymbol{X}}_0=\boldsymbol{X}_1^*,\mu=\mu^*,\bar{\delta}_1=0}=\frac{\partial v_{1\mathrm{c}}}{\partial\bar{\delta}_1}\Big|_{\overline{\boldsymbol{X}}_0=\boldsymbol{X}_1^*,\mu=\mu^*}=v_{1\mathrm{c},\boldsymbol{X}}\boldsymbol{F}_{1s}^*=a_{1\mathrm{c}}^*.
\end{aligned}$$

由于 $\boldsymbol{X}_1^*$ 位于碰撞面 Σ_1上, 有 $H_1(\boldsymbol{X}_1^*,\mu^*)=0$. $\overline{\boldsymbol{X}}_0$ 位于截面 Π_1上, 即存在 $v_{1\mathrm{c}}(\overline{\boldsymbol{X}}_0,\mu)=0$. 将 $v_{1\mathrm{c}}(\overline{\boldsymbol{X}}_0,\mu)$Taylor 展开, 并利用$v_{1\mathrm{c}}(\overline{\boldsymbol{X}}_0,\mu)=0$, 有

$$v_{1\mathrm{c}}(\overline{\boldsymbol{X}}_0,\mu)=v_{1\mathrm{c},\boldsymbol{X}}(\overline{\boldsymbol{X}}_0-\boldsymbol{X}_1^*)+v_{1\mathrm{c},\mu}(\mu-\mu^*)+h.o.t.=0.$$

此外, $\boldsymbol{\Phi}_{1,\overline{\boldsymbol{X}}_0}\big|_{\overline{\boldsymbol{X}}_0=\boldsymbol{X}^*,\ \mu=\mu^*,t=0}=\boldsymbol{I},\boldsymbol{\Phi}_{1,\mu}\big|_{\overline{\boldsymbol{X}}_0=\boldsymbol{X}^*,\mu=\mu^*,t=0}=0$. 利用这些条件, 方程 (20) 可化简为

$$H_{1,\boldsymbol{X}}(\overline{\boldsymbol{X}}_0-\boldsymbol{X}_1^*)+H_{1,\mu}(\mu-\mu^*)+\frac{1}{2}a_{1\mathrm{c}}^*\bar{\delta}_1^2+h.o.t.=H_1(\overline{\boldsymbol{X}}_0,\mu)+\frac{1}{2}a_{1\mathrm{c}}^*\bar{\delta}_1^2+h.o.t.=0. \tag{21}$$

根据方程 (21)可解得时间 $\bar{\delta}_1$为

$$\bar{\delta}_1=-\sqrt{\frac{-2H_1(\overline{\boldsymbol{X}}_0,\mu)}{a_{1\mathrm{c}}^*}}. \tag{22}$$

第二步, 从 $\overline{\boldsymbol{X}}_1$到 $\overline{\boldsymbol{X}}_2$, 计算所用的时间 $\bar{\delta}_2$.

类似式 (19)将流函数 $\boldsymbol{\Phi}_2(\overline{\boldsymbol{X}}_1,\mu,\bar{\delta}_2)$一阶 Taylor 展开有

$$\overline{\boldsymbol{X}}_2=\boldsymbol{\Phi}_2(\overline{\boldsymbol{X}}_1,\mu,\bar{\delta}_2)=\overline{\boldsymbol{X}}_1+\boldsymbol{F}_2^*\bar{\delta}_2+h.o.t.. \tag{23}$$

因为 $\overline{\boldsymbol{X}}_2$ 在分界面 Σ_1上, 存在 $H_1(\overline{\boldsymbol{X}}_2,\mu)=0$. 类似 Taylor 展开式 (20), 将 $H_1(\overline{\boldsymbol{X}}_2,\mu)$Taylor 展开并利用 $H_1(\overline{\boldsymbol{X}}_2,\mu)=0$有

$$H_1(\overline{\boldsymbol{X}}_2,\mu)=H_1(\boldsymbol{\Phi}_2(\overline{\boldsymbol{X}}_1,\mu,\bar{\delta}_2),\mu)=G_2(\overline{\boldsymbol{X}}_1,\mu,\bar{\delta}_2)=$$
$$G_2(\boldsymbol{X}_1^*,\mu^*,0)+G_{2,\overline{\boldsymbol{X}}_1}\big|_{\overline{\boldsymbol{X}}_1=\boldsymbol{X}_1^*,\mu=\mu^*,\bar{\delta}_2=0}(\overline{\boldsymbol{X}}_1-\boldsymbol{X}_1^*)+G_{2,\mu}\big|_{\overline{\boldsymbol{X}}_1=\boldsymbol{X}_1^*,\mu=\mu^*,\bar{\delta}_2=0}(\mu-\mu^*)+$$
$$G_{2,\bar{\delta}_2}\big|_{\overline{\boldsymbol{X}}_1=\boldsymbol{X}_1^*,\mu=\mu^*,\bar{\delta}_2=0}\bar{\delta}_2+G_{2,\overline{\boldsymbol{X}}_1,\bar{\delta}_2}\big|_{\overline{\boldsymbol{X}}_1=\boldsymbol{X}_1^*,\mu=\mu^*,\bar{\delta}_2=0}(\overline{\boldsymbol{X}}_1-\boldsymbol{X}_1^*)\bar{\delta}_2+$$
$$G_{2,\mu,\bar{\delta}_2}\big|_{\overline{\boldsymbol{X}}_1=\boldsymbol{X}_1^*,\mu=\mu^*,\bar{\delta}_2=0}(\mu-\mu^*)\bar{\delta}_2+G_{2,\overline{\boldsymbol{X}}_1,\overline{\boldsymbol{X}}_1}\big|_{\overline{\boldsymbol{X}}_1=\boldsymbol{X}_1^*,\mu=\mu^*,\bar{\delta}_2=0}(\overline{\boldsymbol{X}}_1-\boldsymbol{X}_1^*)^2+$$
$$G_{1,\mu,\mu}\big|_{\overline{\boldsymbol{X}}_1=\boldsymbol{X}_1^*,\mu=\mu^*,\bar{\delta}_2=0}(\mu-\mu^*)^2+\frac{1}{2}G_{2,\bar{\delta}_2,\bar{\delta}_2}\big|_{\overline{\boldsymbol{X}}_1=\boldsymbol{X}_1^*,\mu=\mu^*,\bar{\delta}_2=0}\bar{\delta}_2^2+h.o.t.=0,\tag{24}$$

式中

$$G_2(\boldsymbol{X}_1^*,\mu^*,0)=H_1(\boldsymbol{X}_1^*,\mu^*),\ G_{2,\overline{\boldsymbol{X}}_1}\big|_{\overline{\boldsymbol{X}}_1=\boldsymbol{X}_1^*,\mu=\mu^*,\bar{\delta}_2=0}=H_{1,\boldsymbol{X}}\boldsymbol{\Phi}_{2,\overline{\boldsymbol{X}}_1},$$
$$G_{2,\mu}\big|_{\overline{\boldsymbol{X}}_1=\boldsymbol{X}_1^*,\mu=\mu^*,\bar{\delta}_2=0}=H_{1,\mu}(\boldsymbol{\Phi}_{2,\mu}+\boldsymbol{I}),\ G_{2,\bar{\delta}_1}\big|_{\overline{\boldsymbol{X}}_1=\boldsymbol{X}_1^*,\mu=\mu^*,\bar{\delta}_2=0}=H_{1,\boldsymbol{X}}\boldsymbol{F}_2^*=v_{1\mathrm{u}},$$
$$G_{2,\overline{\boldsymbol{X}}_1,\bar{\delta}_2}\big|_{\overline{\boldsymbol{X}}_1=\boldsymbol{X}_1^*,\mu=\mu^*,\bar{\delta}_2=0}=\frac{\partial v_{1\mathrm{u}}}{\partial\boldsymbol{X}}\bigg|_{\overline{\boldsymbol{X}}_1=\boldsymbol{X}_1^*,\mu=\mu^*}=v_{1\mathrm{u},\boldsymbol{X}},\ G_{2,\mu,\bar{\delta}_2}\big|_{\overline{\boldsymbol{X}}_1=\boldsymbol{X}_1^*,\mu=\mu^*,\bar{\delta}_2=0}=\frac{\partial v_{1\mathrm{u}}}{\partial\mu}\bigg|_{\overline{\boldsymbol{X}}_1=\boldsymbol{X}_1^*,\mu=\mu^*}=v_{1\mathrm{u},\mu},$$
$$G_{2,\overline{\boldsymbol{X}}_1,\overline{\boldsymbol{X}}_1}\big|_{\overline{\boldsymbol{X}}_1=\boldsymbol{X}_1^*,\mu=\mu^*,\bar{\delta}_2=0}=\frac{\partial H_{1,\boldsymbol{X}}\boldsymbol{\Phi}_{2,\overline{\boldsymbol{X}}_1}}{\partial\overline{\boldsymbol{X}}_1}\bigg|_{\overline{\boldsymbol{X}}_1=\boldsymbol{X}_1^*,\mu=\mu^*},\ G_{1,\mu,\mu}\big|_{\overline{\boldsymbol{X}}_1=\boldsymbol{X}_1^*,\mu=\mu^*,\bar{\delta}_2=0}=\frac{\partial H_{1,\mu}(\boldsymbol{\Phi}_{2,\mu}+\boldsymbol{I})}{\partial\mu}\bigg|_{\overline{\boldsymbol{X}}_1=\boldsymbol{X}_1^*,\mu=\mu^*},$$
$$G_{2,\bar{\delta}_2,\bar{\delta}_2}\big|_{\overline{\boldsymbol{X}}_1=\boldsymbol{X}_1^*,\mu=\mu^*,\bar{\delta}_2=0}=\frac{\partial v_{1\mathrm{u}}}{\partial\bar{\delta}_2}\bigg|_{\overline{\boldsymbol{X}}_1=\boldsymbol{X}_1^*,\mu=\mu^*}=v_{1\mathrm{u},\boldsymbol{X}}\boldsymbol{F}_2^*=a_{1\mathrm{u}}^*.$$

利用这些条件, 方程 (24)可化简为

$$v_{1\mathrm{u},\boldsymbol{X}}\boldsymbol{F}_{1s}^*\bar{\delta}_1\bar{\delta}_2+\frac{1}{2}a_{1\mathrm{u}}^*\bar{\delta}_2^2+h.o.t.=0.\tag{25}$$

根据方程 (25)可得到从 $\overline{\boldsymbol{X}}_1$到 $\overline{\boldsymbol{X}}_2$的时间 $\bar{\delta}_2$为

$$\bar{\delta}_2=-\frac{2v_{1\mathrm{u},\boldsymbol{X}}\boldsymbol{F}_{1s}^*}{a_{1\mathrm{u}}^*}\bar{\delta}_1.\tag{26}$$

第三步, 从 $\overline{\boldsymbol{X}}_2$到 $\overline{\boldsymbol{X}}_3$的时间记为 $-\bar{\delta}_3$, 计算时间 $\bar{\delta}_3$.

类似式 (19), 将流函数 $\boldsymbol{\Phi}_1(\overline{\boldsymbol{X}}_2,\mu,-\bar{\delta}_3)$ 一阶 Taylor 展开并利用式 (19)、(23)可得

$$\overline{\boldsymbol{X}}_3=\boldsymbol{\Phi}_1(\overline{\boldsymbol{X}}_2,\mu,-\bar{\delta}_3)=\overline{\boldsymbol{X}}_2-\boldsymbol{F}_{1s}^*\bar{\delta}_3+h.o.t.=\overline{\boldsymbol{X}}_0+\boldsymbol{F}_{1s}^*\bar{\delta}_1+\boldsymbol{F}_2^*\bar{\delta}_2-\boldsymbol{F}_{1s}^*\bar{\delta}_3+h.o.t..\tag{27}$$

因为 $\overline{\boldsymbol{X}}_3$位于截面 Π_1上, 有 $v_{1\mathrm{c}}(\boldsymbol{X}_3,\mu)=0$, 对 $v_{1\mathrm{c}}(\overline{\boldsymbol{X}}_3,\mu)$一阶 Taylor 展开得到

$$v_{1\mathrm{c}}(\overline{\boldsymbol{X}}_3,\mu)=v_{1\mathrm{c},\boldsymbol{X}}(\overline{\boldsymbol{X}}_3-\boldsymbol{X}_1^*)+v_{1\mathrm{c},\mu}(\mu-\mu^*)+h.o.t.=0.\tag{28}$$

将式 (27)代入方程 (28)可得

$$v_{1\mathrm{c}}(\overline{\boldsymbol{X}}_3,\mu)=v_{1\mathrm{c},\boldsymbol{X}}(\overline{\boldsymbol{X}}_0-\boldsymbol{X}_1^*)+v_{1\mathrm{c},\boldsymbol{X}}\boldsymbol{F}_{1s}^*\bar{\delta}_1+v_{1\mathrm{c},\boldsymbol{X}}\boldsymbol{F}_2^*\bar{\delta}_2-v_{1\mathrm{c},\boldsymbol{X}}\boldsymbol{F}_{1s}^*\bar{\delta}_3+v_{1\mathrm{c},\mu}(\mu-\mu^*)+h.o.t.=$$
$$v_{1\mathrm{c},\boldsymbol{X}}\boldsymbol{F}_{1s}^*\bar{\delta}_1+v_{1\mathrm{c},\boldsymbol{X}}\boldsymbol{F}_2^*\bar{\delta}_2-v_{1\mathrm{c},\boldsymbol{X}}\boldsymbol{F}_{1s}^*\bar{\delta}_3=0.\tag{29}$$

根据式 (29)得到从 $\overline{\boldsymbol{X}}_2$到 $\overline{\boldsymbol{X}}_3$的时间 $\bar{\delta}_3$为

$$\bar{\delta}_3=\frac{v_{1\mathrm{c},\boldsymbol{X}}\boldsymbol{F}_{1s}^*\bar{\delta}_1+v_{1\mathrm{c},\boldsymbol{X}}\boldsymbol{F}_2^*\bar{\delta}_2}{v_{1\mathrm{c},\boldsymbol{X}}\boldsymbol{F}_{1s}^*}.\tag{30}$$

最后将式 (26)、(30)代入式 (27)得到

$$\overline{\boldsymbol{X}}_3=\overline{\boldsymbol{X}}_0+\boldsymbol{\xi}_1\bar{\delta}_1,\tag{31}$$

其中 $\boldsymbol{\xi}_1=2\left(\boldsymbol{F}_{1s}^*\dfrac{v_{1\mathrm{c},\boldsymbol{X}}\boldsymbol{F}_2^*}{v_{1\mathrm{c},\boldsymbol{X}}\boldsymbol{F}_{1s}^*}-\boldsymbol{F}_2^*\right)\dfrac{v_{1\mathrm{u},\boldsymbol{X}}\boldsymbol{F}_{1s}^*}{a_{1\mathrm{u}}^*}$.

根据上面的推导可得到如下低阶范式不连续映射 $\boldsymbol{P}_{\mathrm{PDM1}}$:

$$\boldsymbol{P}_{\mathrm{PDM1}}(\boldsymbol{X}_1,\mu)=\begin{cases}\boldsymbol{X}_1, & H_1(\boldsymbol{X}_1,\mu)<0,\\ \boldsymbol{X}_1+\boldsymbol{\xi}_1\bar{\delta}_1+h.o.t., & H_1(\boldsymbol{X}_1,\mu)\geqslant 0,\end{cases}\tag{32}$$

这里 $\boldsymbol{X}_1$为图 3 中的 $\overline{\boldsymbol{X}}_0$.类似 $\boldsymbol{P}_{\mathrm{PDM1}}$ 的推导, 可得到如下低阶不连续映射 $\boldsymbol{P}_{\mathrm{PDM2}}$:

$$\boldsymbol{P}_{\mathrm{PDM2}}(\boldsymbol{X}_2,\mu)=\begin{cases}\boldsymbol{X}_2, & H_2(\boldsymbol{X}_2,\mu)\geqslant 0,\\ \boldsymbol{X}_2+\boldsymbol{\xi}_2\bar{t}_1+h.o.t., & H_2(\boldsymbol{X}_2,\mu)<0,\end{cases}\tag{33}$$

这里 $\boldsymbol{X}_2$为图 3 中的 $\tilde{\boldsymbol{X}}_0$, 其中

$$\begin{aligned}&\boldsymbol{\xi}_2=2\left(\boldsymbol{F}_{1x}^*\frac{v_{2\mathrm{c},\boldsymbol{X}}\boldsymbol{F}_3^*}{v_{2\mathrm{c},\boldsymbol{X}}\boldsymbol{F}_{1x}^*}-\boldsymbol{F}_3^*\right)\frac{v_{2\mathrm{d},\boldsymbol{X}}\boldsymbol{F}_{1x}^*}{a_{2\mathrm{d}}^*},\ \bar{t}_1=-\sqrt{\frac{-2H_2(\tilde{\boldsymbol{X}}_0,\mu)}{a_{2\mathrm{c}}^*}},\ v_{2\mathrm{c}}=H_{2,\boldsymbol{X}}\boldsymbol{F}_{1x}^*,\\ &v_{2\mathrm{c},\boldsymbol{X}}=\left.\frac{\partial v_{2\mathrm{c}}}{\partial\boldsymbol{X}}\right|_{\boldsymbol{X}=\boldsymbol{X}^*,\,\mu=\mu^*},\ v_{2\mathrm{c},\mu}=\left.\frac{\partial v_{2\mathrm{c}}}{\partial\mu}\right|_{\boldsymbol{X}=\boldsymbol{X}^*,\mu=\mu^*},\ a_{2\mathrm{c}}^*=H_{2,\boldsymbol{X}}\boldsymbol{F}_{1x,\boldsymbol{X}}^*\boldsymbol{F}_{1x}^*=v_{2\mathrm{c},\boldsymbol{X}}^*\boldsymbol{F}_{1x}^*,\\ &v_{2\mathrm{d}}=H_{2,\boldsymbol{X}}\boldsymbol{F}_3^*,\ v_{2\mathrm{d},\boldsymbol{X}}=\left.\frac{\partial v_{2\mathrm{d}}}{\partial\boldsymbol{X}}\right|_{\boldsymbol{X}=\boldsymbol{X}^*,\mu=\mu^*},\ v_{2\mathrm{d},\mu}=\left.\frac{\partial v_{2\mathrm{d}}}{\partial\mu}\right|_{\boldsymbol{X}=\boldsymbol{X}^*,\mu=\mu^*},\ a_{2\mathrm{d}}^*=H_{2,\boldsymbol{X}}\boldsymbol{F}_{3,\boldsymbol{X}}^*\boldsymbol{F}_3^*=v_{2\mathrm{d},\boldsymbol{X}}^*\boldsymbol{F}_3^*,\\ &H_2(\tilde{\boldsymbol{X}}_0,\mu)=H_{2,\boldsymbol{X}}(\tilde{\boldsymbol{X}}_0-\boldsymbol{X}_2^*)+H_{2,\mu}(\mu-\mu^*).\end{aligned}\tag{34}$$

这里讨论 $\boldsymbol{X}_1^*$和 $\boldsymbol{X}_2^*$是一对对称的擦边点. 依据通解 (6)定义两个光滑的 Poincaré 映射:

$$\boldsymbol{P}_{1N}:\Pi_1\to\Pi_2,\ \boldsymbol{P}_{2N}:\Pi_2\to\Pi_1,$$

使得 $\boldsymbol{P}_{1N}(\boldsymbol{X}_1^*,\mu^*)=(\boldsymbol{X}_2^*,\mu^*),\boldsymbol{P}_{2N}(\boldsymbol{X}_2^*,\mu^*)=(\boldsymbol{X}_1^*,\mu^*)$. 为了研究局部的擦边分岔, 将 $\boldsymbol{P}_{1N}$, $\boldsymbol{P}_{2N}$分别在 $(\boldsymbol{X}_1^*,\mu^*)$, $(\boldsymbol{X}_2^*,\mu^*)$ Taylor 展开:

$$\boldsymbol{P}_{1N}=\boldsymbol{X}_2^*+\boldsymbol{N}_1(\boldsymbol{X}_1-\boldsymbol{X}_1^*)+\boldsymbol{M}_1(\mu-\mu^*),\ \boldsymbol{P}_{2N}=\boldsymbol{X}_1^*+\boldsymbol{N}_2(\boldsymbol{X}_2-\boldsymbol{X}_2^*)+\boldsymbol{M}_2(\mu-\mu^*),\tag{35}$$

这里

$$\boldsymbol{N}_1=\left.\frac{\partial\boldsymbol{P}_{1N}}{\partial\boldsymbol{X}}\right|_{\boldsymbol{X}_1=\boldsymbol{X}_1^*},\ \boldsymbol{N}_2=\left.\frac{\partial\boldsymbol{P}_{2N}}{\partial\boldsymbol{X}}\right|_{\boldsymbol{X}_2=\boldsymbol{X}_2^*},$$

$$\boldsymbol{M}_1=\left.\frac{\partial\boldsymbol{P}_{1N}}{\partial\mu}\right|_{\mu=\mu^*},\ \boldsymbol{M}_2=\left.\frac{\partial\boldsymbol{P}_{2N}}{\partial\mu}\right|_{\mu=\mu^*}.$$

结合不连续映射 (32)、(33)和光滑映射 (35), 建立如下复合的擦边范式映射:

$$\boldsymbol{P}=\boldsymbol{P}_{2N}\circ\boldsymbol{P}_{\mathrm{PDM2}}\circ\boldsymbol{P}_{1N}\circ\boldsymbol{P}_{\mathrm{PDM1}}.\tag{36}$$

接下来讨论复合映射 (36)的表达式.

1) 如果 $H_1(\boldsymbol{X}_1,\mu)<0$, 此时 $\boldsymbol{P}_{\mathrm{PDM1}}$ 为单位矩阵, 那么

$$\boldsymbol{X}_2=\boldsymbol{P}_{1N}\circ\boldsymbol{P}_{\mathrm{PDM1}}=\boldsymbol{X}_2^*+\boldsymbol{N}_1(\boldsymbol{X}_1-\boldsymbol{X}_1^*)+\boldsymbol{M}_1(\mu-\mu^*)+h.o.t..\tag{37}$$

① 如果 $H_2(\boldsymbol{X}_2,\mu)\geqslant 0$, 此时 $\boldsymbol{P}_{\mathrm{PDM2}}$ 为单位矩阵, 该情况表示小球与上下方约束均不碰撞:

$$\boldsymbol{P}=\boldsymbol{P}_{2N}\circ\boldsymbol{P}_{\mathrm{PDM2}}\circ\boldsymbol{P}_{1N}\circ\boldsymbol{P}_{\mathrm{PDM1}}=\boldsymbol{X}_1^*+\boldsymbol{N}_2(\boldsymbol{X}_2-\boldsymbol{X}_2^*)+\boldsymbol{M}_2(\mu-\mu^*)+h.o.t..\tag{38}$$

② 如果 $H_2(\boldsymbol{X}_2,\mu)<0$, 该情况表示小球与上方约束不碰撞, 与下方约束发生碰撞:

$$\boldsymbol{P}=\boldsymbol{P}_{2N}\circ\boldsymbol{P}_{\mathrm{PDM2}}\circ\boldsymbol{P}_{1N}\circ\boldsymbol{P}_{\mathrm{PDM1}}=\boldsymbol{X}_1^*+\boldsymbol{N}_2(\boldsymbol{P}_{\mathrm{PDM2}}(\boldsymbol{X}_2)-\boldsymbol{X}_2^*)+\boldsymbol{M}_2(\mu-\mu^*)+h.o.t..\tag{39}$$

2) 如果 $H_1(\boldsymbol{X}_1,\mu)\geqslant 0$, 那么

$$\boldsymbol{X}_2=\boldsymbol{P}_{1N}\circ\boldsymbol{P}_{\mathrm{PDM1}}=\boldsymbol{X}_2^*+\boldsymbol{N}_1(\boldsymbol{P}_{\mathrm{PDM1}}-\boldsymbol{X}_1^*)+\boldsymbol{M}_1(\mu-\mu^*)+h.o.t..\tag{40}$$

① 如果 $H_2(\boldsymbol{X}_2,\mu)\geqslant 0$, 此时 $\boldsymbol{P}_{\mathrm{PDM2}}$ 为单位矩阵, 该情况表示小球与上方约束发生碰撞, 与下方约束不发生碰撞:

$$\boldsymbol{P}=\boldsymbol{P}_{2N}\circ\boldsymbol{P}_{\mathrm{PDM2}}\circ\boldsymbol{P}_{1N}\circ\boldsymbol{P}_{\mathrm{PDM1}}=\boldsymbol{X}_1^*+\boldsymbol{N}_2(\boldsymbol{X}_2-\boldsymbol{X}_2^*)+\boldsymbol{M}_2(\mu-\mu^*)+h.o.t..\tag{41}$$

② 如果 $H_2(\boldsymbol{X}_2,\mu)<0$, 该情况表示小球既与上方约束碰撞, 又与下方约束发生碰撞:

$$\boldsymbol{P}=\boldsymbol{P}_{2N}\circ\boldsymbol{P}_{\mathrm{PDM2}}\circ\boldsymbol{P}_{1N}\circ\boldsymbol{P}_{\mathrm{PDM1}}=\boldsymbol{X}_1^*+\boldsymbol{N}_2(\boldsymbol{P}_{\mathrm{PDM2}}(\boldsymbol{X}_2)-\boldsymbol{X}_2^*)+\boldsymbol{M}_2(\mu-\mu^*)+h.o.t..\tag{42}$$

将不连续映射 (32)和 (33)代入到式 (38)、(39)、(41)和 (42)中, 可得如命题 2 所示的低阶复合范式映射.

命题 2 双侧弹性约束悬臂梁系统 (2) 以零速度为截面的低阶的分段复合范式映射为

$$\boldsymbol{P}(\hat{\boldsymbol{X}}_1,\hat{\mu})=\begin{cases}\boldsymbol{X}_1^*+\boldsymbol{N}_2\boldsymbol{N}_1\hat{\boldsymbol{X}}_1+\boldsymbol{N}_2\boldsymbol{M}_1\hat{\mu}+\boldsymbol{M}_2\hat{\mu}+h.o.t., & H_1(\hat{\boldsymbol{X}}_1,\hat{\mu})<0,\ H_2(\hat{\boldsymbol{X}}_2,\hat{\mu})\geqslant 0,\\ \boldsymbol{X}_1^*+\boldsymbol{N}_2\boldsymbol{N}_1\hat{\boldsymbol{X}}_1+\boldsymbol{N}_2\boldsymbol{M}_1\hat{\mu}+\boldsymbol{N}_2\xi_2\bar{t}_1+\boldsymbol{M}_2\hat{\mu}+h.o.t., & H_1(\hat{\boldsymbol{X}}_1,\hat{\mu})<0,\ H_2(\hat{\boldsymbol{X}}_2,\hat{\mu})<0,\\ \boldsymbol{X}_1^*+\boldsymbol{N}_2\boldsymbol{N}_1\hat{\boldsymbol{X}}_1+\boldsymbol{N}_2\boldsymbol{N}_1\xi_1\bar{\delta}_1+\boldsymbol{N}_2\boldsymbol{M}_1\hat{\mu}+\boldsymbol{M}_2\hat{\mu}+h.o.t., & H_1(\hat{\boldsymbol{X}}_1,\hat{\mu})\geqslant 0,\ H_2(\hat{\boldsymbol{X}}_2,\hat{\mu})\geqslant 0,\\ \boldsymbol{X}_1^*+\boldsymbol{N}_2\boldsymbol{N}_1\hat{\boldsymbol{X}}_1+\boldsymbol{N}_2\boldsymbol{N}_1\xi_1\bar{\delta}_1+\boldsymbol{N}_2\boldsymbol{M}_1\hat{\mu}+\boldsymbol{N}_2\xi_2\bar{t}_1+\boldsymbol{M}_2\hat{\mu}+h.o.t., & H_1(\hat{\boldsymbol{X}}_1,\hat{\mu})\geqslant 0,\ H_2(\hat{\boldsymbol{X}}_2,\hat{\mu})<0,\end{cases}\tag{43}$$

其中

$$\hat{\mu}=\mu-\mu^*,\ \hat{\boldsymbol{X}}_i=\boldsymbol{X}_i-\boldsymbol{X}_i^*\qquad(i=1,2).$$

3.2　高阶复合范式映射

这一小节推导系统 (2)擦边轨道附近的高阶范式映射. 为了推导高阶范式, 需将一般流函数$\boldsymbol{\Phi}_i(\boldsymbol{X},\mu,\delta)(i=1,2,3)$在 $\boldsymbol{X}=\boldsymbol{X}^*$和 $\mu=\mu^*$ 处对时间 δ展开到二阶项, 有

$$\boldsymbol{\Phi}_i(\boldsymbol{X},\mu,\delta)=\boldsymbol{X}+\boldsymbol{F}_i^*\delta+\boldsymbol{F}_{i,\boldsymbol{X}}{}^*(\boldsymbol{X}-\boldsymbol{X}^*)\delta+\boldsymbol{F}_{i,\mu}^*(\mu-\mu^*)\delta+\frac{1}{2}\boldsymbol{F}_{i,\boldsymbol{X}}^*\boldsymbol{F}_i^*\delta^2+h.o.t.,\tag{44}$$

式中 $\boldsymbol{F}_i^*=\boldsymbol{F}_i(\boldsymbol{X}^*,\mu^*)$表示擦边点 $\boldsymbol{X}^*$处的向量场, $\boldsymbol{F}_{i,\boldsymbol{X}}{}^*=\left.\dfrac{\partial\boldsymbol{F}_i(\boldsymbol{X},\mu)}{\partial\boldsymbol{X}}\right|_{\boldsymbol{X}=\boldsymbol{X}^*,\mu=\mu^*}$, $\boldsymbol{F}_{i,\mu}^*=\left.\dfrac{\partial\boldsymbol{F}_i(\boldsymbol{X},\mu)}{\partial\mu}\right|_{\boldsymbol{X}=\boldsymbol{X}^*,\mu=\mu^*}$.

区别于低阶范式推导, 将式 (28)中 $v_{1c}(\overline{\boldsymbol{X}}_3,\mu)$二阶 Taylor 展开有

$$\begin{aligned}v_{1c}(\overline{\boldsymbol{X}}_3,\mu)=&v_{1c,\boldsymbol{X}}(\overline{\boldsymbol{X}}_2-\boldsymbol{X}_1^*)+v_{1c,\mu}(\mu-\mu^*)-v_{1c,\boldsymbol{X}}\boldsymbol{F}_{1s}^*\tilde{\delta}_3-v_{1c,\boldsymbol{X}}\boldsymbol{F}_{1s,\boldsymbol{X}}^*(\overline{\boldsymbol{X}}_2-\boldsymbol{X}_1^*)\tilde{\delta}_3-\\ &v_{1c,\boldsymbol{X}}\boldsymbol{F}_{1s,\mu}^*(\mu-\mu^*)\tilde{\delta}_3+\frac{1}{2}v_{1c,\boldsymbol{X}}(\boldsymbol{F}_{1s,\boldsymbol{X}}^*\boldsymbol{F}_{1s}^*)\tilde{\delta}_3^2+h.o.t.=0.\end{aligned}\tag{45}$$

基于式 (24)、(44)和 (45)可知 $\tilde{\delta}_i(i=2,3)$是关于自变量 $\tilde{\delta}_1,\overline{\boldsymbol{X}}_0,\mu$的函数, 将其表示为 $\tilde{\delta}_i=\tilde{\delta}_i(\tilde{\delta}_1,\overline{\boldsymbol{X}}_0,\mu)$, 并对自变量二阶 Taylor 展开有

$$\begin{cases}\tilde{\delta}_2(\tilde{\delta}_1,\overline{\boldsymbol{X}}_0,\mu)=f_0\tilde{\delta}_1+\boldsymbol{f}_1(\overline{\boldsymbol{X}}_0-\boldsymbol{X}_1^*)\tilde{\delta}_1+f_2(\mu-\mu^*)\tilde{\delta}_1+f_3\tilde{\delta}_1^2+h.o.t.,\\ \tilde{\delta}_3(\tilde{\delta}_1,\overline{\boldsymbol{X}}_0,\mu)=e_0\tilde{\delta}_1+\boldsymbol{e}_1(\overline{\boldsymbol{X}}_0-\boldsymbol{X}_1^*)\tilde{\delta}_1+e_2(\mu-\mu^*)\tilde{\delta}_1+e_3\tilde{\delta}_1^2+h.o.t..\end{cases}\tag{46}$$

基于以上展开式, 类似 3.1小节的步骤可得如下高阶范式不连续映射 $\boldsymbol{P}_{\mathrm{PDM1}}$和 $\boldsymbol{P}_{\mathrm{PDM2}}$:

$$\boldsymbol{P}_{\mathrm{PDM1}}(\boldsymbol{X}_1,\mu)=\begin{cases}\boldsymbol{X}_1, & H_1(\boldsymbol{X}_1,\mu)<0,\\ \boldsymbol{X}_1+\boldsymbol{\alpha}_1\tilde{\delta}_1+\boldsymbol{\alpha}_2(\boldsymbol{X}_1-\boldsymbol{X}_1^*)\tilde{\delta}_1+\boldsymbol{\alpha}_3(\mu-\mu^*)\tilde{\delta}_1+\boldsymbol{\alpha}_4\tilde{\delta}_1^2+h.o.t., & H_1(\boldsymbol{X}_1,\mu)\geqslant 0,\end{cases}\tag{47}$$

$$\boldsymbol{P}_{\mathrm{PDM2}}(\boldsymbol{X}_2,\mu)=\begin{cases}\boldsymbol{X}_2, & H_2(\boldsymbol{X}_2,\mu)\geqslant 0,\\ \boldsymbol{X}_2+\boldsymbol{\beta}_1\tilde{t}_1+\boldsymbol{\beta}_2(\boldsymbol{X}_2-\boldsymbol{X}_2^*)\tilde{t}_1+\boldsymbol{\beta}_3(\mu-\mu^*)\tilde{t}_1+\boldsymbol{\beta}_4\tilde{t}_1^2+h.o.t., & H_2(\boldsymbol{X}_2,\mu)<0,\end{cases}\tag{48}$$

其中系数 $\boldsymbol{\alpha}_i$和 $\boldsymbol{\beta}_i(i=1,2,3,4)$的详细表达式见附录.

将不连续映射 (47)和 (48)代入到式 (38)、(39)、(41)和 (42)可得到如命题 3 所示的高阶复合范式映射.

命题 3　双侧弹性约束悬臂梁系统 (2) 以零速度为截面的高阶分段复合范式映射为

$$\boldsymbol{P}(\hat{\boldsymbol{X}}_1,\hat{\mu})=\begin{cases}\boldsymbol{X}_1^*+\boldsymbol{N}_2\boldsymbol{N}_1\hat{\boldsymbol{X}}_1+\boldsymbol{N}_2\boldsymbol{M}_1\hat{\mu}+\boldsymbol{M}_2\hat{\mu}+h.o.t., & H_1(\hat{\boldsymbol{X}}_1,\hat{\mu})<0,\ H_2(\hat{\boldsymbol{X}}_2,\hat{\mu})\geqslant 0,\\ \boldsymbol{X}_1^*+\boldsymbol{N}_2\boldsymbol{N}_1\hat{\boldsymbol{X}}_1+\boldsymbol{N}_2\boldsymbol{M}_1\hat{\mu}+\boldsymbol{N}_2\boldsymbol{\beta}_1\tilde{t}_1+\boldsymbol{N}_2\boldsymbol{N}_1\boldsymbol{\beta}_2\hat{\boldsymbol{X}}_1\tilde{t}_1+\boldsymbol{N}_2\boldsymbol{\beta}_3\hat{\mu}\tilde{t}_1+\boldsymbol{N}_2\boldsymbol{\beta}_4\tilde{t}_1^2+\\ \quad\boldsymbol{M}_2\hat{\mu}+h.o.t., & H_1(\hat{\boldsymbol{X}}_1,\hat{\mu})<0,\ H_2(\hat{\boldsymbol{X}}_2,\hat{\mu})<0,\\ \boldsymbol{X}_1^*+\boldsymbol{N}_2\boldsymbol{N}_1\hat{\boldsymbol{X}}_1+\boldsymbol{N}_2\boldsymbol{N}_1\boldsymbol{\alpha}_1\tilde{\delta}_1+\boldsymbol{N}_2\boldsymbol{N}_1\boldsymbol{\alpha}_2\hat{\boldsymbol{X}}_1\tilde{\delta}_1+\boldsymbol{N}_2\boldsymbol{N}_1\boldsymbol{\alpha}_3\hat{\mu}\tilde{\delta}_1+\boldsymbol{N}_2\boldsymbol{N}_1\boldsymbol{\alpha}_4\tilde{\delta}_1^2+\boldsymbol{N}_2\boldsymbol{M}_1\hat{\mu}+\\ \quad\boldsymbol{M}_2\hat{\mu}+h.o.t., & H_1(\hat{\boldsymbol{X}}_1,\hat{\mu})\geqslant 0,\ H_2(\hat{\boldsymbol{X}}_2,\hat{\mu})\geqslant 0,\\ \boldsymbol{X}_1^*+\boldsymbol{N}_2\boldsymbol{N}_1\hat{\boldsymbol{X}}_1+\boldsymbol{N}_2\boldsymbol{N}_1\boldsymbol{\alpha}_1\tilde{\delta}_1+\boldsymbol{N}_2\boldsymbol{N}_1\boldsymbol{\alpha}_2\hat{\boldsymbol{X}}_1\tilde{\delta}_1+\boldsymbol{N}_2\boldsymbol{N}_1\boldsymbol{\alpha}_3\hat{\mu}\tilde{\delta}_1+\boldsymbol{N}_2\boldsymbol{N}_1\boldsymbol{\alpha}_4\tilde{\delta}_1^2+\boldsymbol{N}_2\boldsymbol{M}_1\hat{\mu}+\\ \quad\boldsymbol{N}_2\boldsymbol{\beta}_1\tilde{t}_1+\boldsymbol{N}_2\boldsymbol{N}_1\boldsymbol{\beta}_2\hat{\boldsymbol{X}}_1\tilde{t}_1+\boldsymbol{N}_2\boldsymbol{N}_1\boldsymbol{\beta}_2\boldsymbol{\alpha}_1\tilde{\delta}_1\tilde{t}_1+\boldsymbol{N}_2\boldsymbol{M}_1\boldsymbol{\beta}_2\hat{\mu}\tilde{t}_1+\\ \quad\boldsymbol{N}_2\boldsymbol{\beta}_3\hat{\mu}\tilde{t}_1+\boldsymbol{N}_2\boldsymbol{\beta}_4\tilde{t}_1^2+\boldsymbol{M}_2\hat{\mu}+h.o.t., & H_1(\hat{\boldsymbol{X}}_1,\hat{\mu})\geqslant 0,\ H_2(\hat{\boldsymbol{X}}_2,\hat{\mu})<0.\end{cases}\tag{49}$$

4　数值仿真

取系统的一组参数 $v=0.1,k_1=k_2=190,w=0.18$, 以间隙 d为分岔参数, 根据命题 1 得到擦边分岔点 $d_0=0.033\,5$. 根据低阶映射 (43) 得到擦边点附近分岔图, 如图 4(a) 所示, 从图 4(a) 可以看到擦边附近没有发生明显的分岔. 根据高阶映射 (49)得到擦边附近分岔图, 如图 4(b) 所示, 从图 4(b) 可以看到系统发生了分岔, 这说明低阶的范式在一定范围内并不能反映原系统的动力学行为.

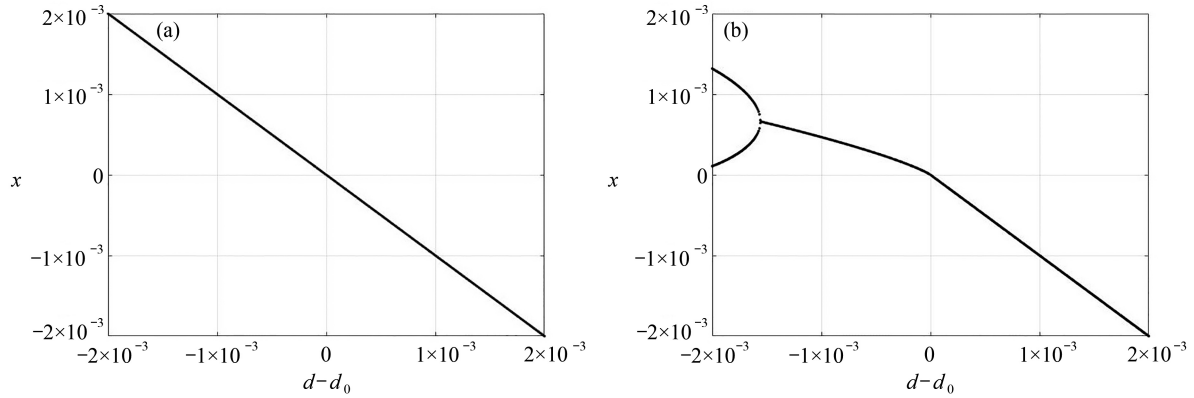

图 4 系统 (2) 擦边轨道附近的分岔图: (a) 基于低阶映射 (43) 得到的擦边轨道附近的分岔图; (b) 基于高阶映射 (49) 得到的擦边轨道附近的分岔图

Fig. 4 The bifurcation diagram of system (2) near the grazing orbit: (a) the bifurcation diagram near the grazing orbit obtained based on low-order mapping (43); (b) the bifurcation diagram near the grazing orbit obtained based on high-order mapping (49)

基于图 4(b) 通过相图进一步来调查擦边附近的动力学行为, 为了方便, 这里以符号 p-q-s 描述系统的碰撞周期运动, 其中 p 表示与上约束面的碰撞次数, q 表示与下约束面的碰撞次数, s表示激振力的周期数. 从图 4(b) 可以看到, 在擦边分岔点 d_0 的右侧, 系统处于稳定的非碰撞单周期运动, 如图 5 所示. 当 $d=d_0$ 时, 系统刚好处于擦边周期运动, 如图 6 所示. 当参数 d穿越分岔点 d_0时, 系统经过擦边分岔进入稳定的 1-1-1 周期运动, 如图 7 所示. 随着参数的进一步减小, 双碰周期一运动发生倍化分岔, 系统进入稳定的 2-2-2 周期运动, 如图 8 所示.

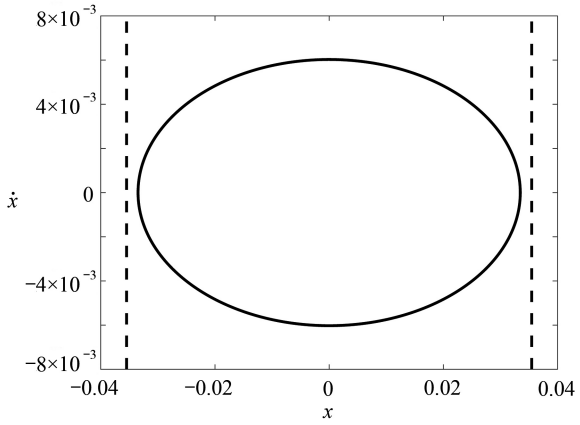

图 5 在 $d=d_0+0.002$处的非碰撞单周期运动

Fig. 5 The non-impact single periodic motion at $d=d_0+0.002$

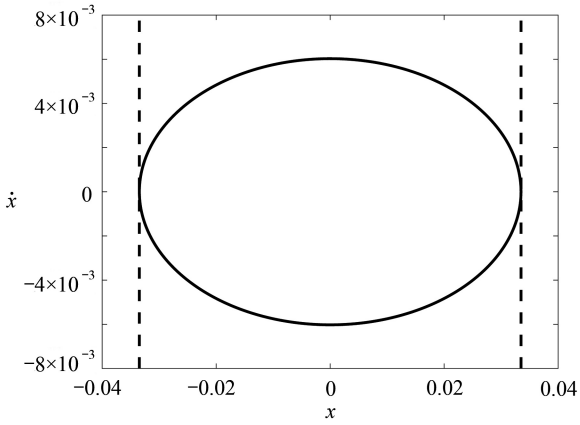

图 6 在 $d=d_0$处的双擦边周期运动

Fig. 6 The double grazing periodic motion at $d=d_0$

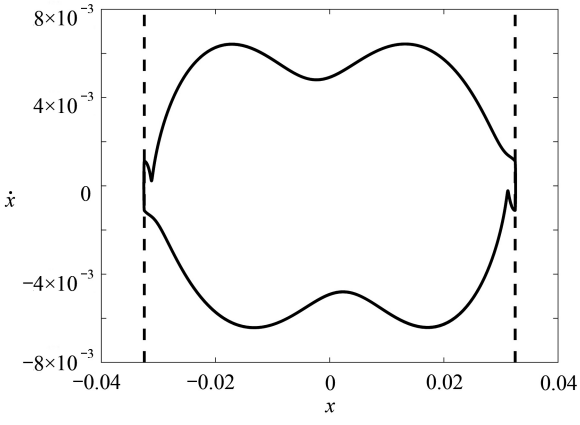

图 7 在 $d=d_0-0.001$处的 1-1-1 碰撞周期运动

Fig. 7 The 1-1-1 impact periodic motion at $d=d_0-0.001$

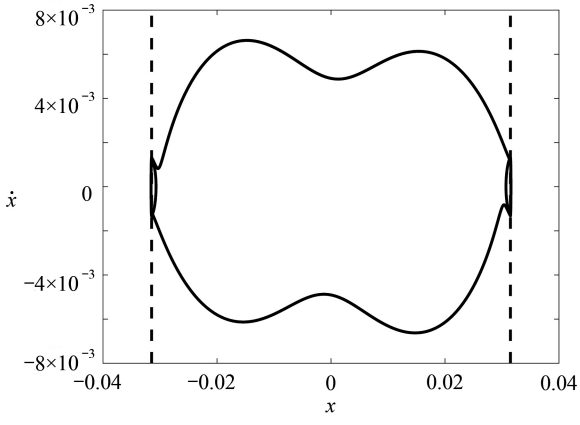

图 8 在 $d=d_0-0.002$处的 2-2-2 碰撞周期运动

Fig. 8 The 2-2-2 impact periodic motion at $d=d_0-0.002$

5 结　论

本文研究了双侧弹性约束的悬臂梁系统的非光滑擦边动力学行为. 在建立速度为零的 Poincaré 截面基础上, 推导了带参数的高阶范式局部不连续映射, 结合不连续映射和光滑映射获得了双擦边运动的高阶复合分段范式映射, 一定程度上解决了低阶范式映射在特定参数域内无法反映原系统擦边分岔特性的问题. 基于高阶的复合映射揭示了悬臂梁擦边附近的局部动力学行为.

附　录

$$f_0=-\frac{2v_{1\mathrm{u},\boldsymbol{X}}\boldsymbol{F}^*_{1s}}{a^*_{1\mathrm{u}}},\ \boldsymbol{f}_1=-\frac{2v_{1\mathrm{u},\boldsymbol{X}}\boldsymbol{F}^*_{1s,\boldsymbol{X}}}{a^*_{1\mathrm{u}}},\ f_2=-\frac{2v_{1\mathrm{u},\boldsymbol{X}}\boldsymbol{F}^*_{1s,\mu}}{a^*_{1\mathrm{u}}},\ f_3=-\frac{v_{1\mathrm{u},\boldsymbol{X}}\boldsymbol{F}^*_{1s,\boldsymbol{X}}\boldsymbol{F}^*_{1s}}{a^*_{1\mathrm{u}}},$$

$$e_0=\frac{v_{1\mathrm{c},\boldsymbol{X}}(\boldsymbol{F}^*_{1s}+\boldsymbol{F}^*_2f_0)}{a^*_{1\mathrm{c}}},\ \boldsymbol{e}_1=\frac{v_{1\mathrm{c},\boldsymbol{X}}(\boldsymbol{F}^*_2\boldsymbol{f}_1+\boldsymbol{F}^*_{1s,\boldsymbol{X}}+\boldsymbol{F}^*_{2,\boldsymbol{X}}f_0-\boldsymbol{F}^*_{1s,\boldsymbol{X}}e_0)}{a^*_{1\mathrm{c}}},$$

$$e_2=\frac{v_{1\mathrm{c},\boldsymbol{X}}(\boldsymbol{F}^*_2f_2+\boldsymbol{F}^*_{1s,\mu}+\boldsymbol{F}^*_{2,\mu}f_0-\boldsymbol{F}^*_{1s,\mu}e_0)}{a^*_{1\mathrm{c}}},$$

$$e_3=\frac{v_{1\mathrm{c},\boldsymbol{X}}}{2a^*_{1\mathrm{c}}}(-2\boldsymbol{F}^*_{1s,\boldsymbol{X}}\boldsymbol{F}^*_2f_0e_0+\boldsymbol{F}^*_{2,\boldsymbol{X}}\boldsymbol{F}^*_2f_0^2-2\boldsymbol{F}^*_{1s,\boldsymbol{X}}\boldsymbol{F}^*_{1s}e_0+2\boldsymbol{F}^*_{2,\boldsymbol{X}}\boldsymbol{F}^*_{1s}f_0+\boldsymbol{F}^*_{1s,\boldsymbol{X}}\boldsymbol{F}^*_{1s}e_0^2+\boldsymbol{F}^*_{1s,\boldsymbol{X}}\boldsymbol{F}^*_{1s}+2\boldsymbol{F}^*_2f_3),$$

$$\boldsymbol{\alpha}_1=\boldsymbol{F}^*_{1s}+\boldsymbol{F}^*_2f_0-\boldsymbol{F}^*_{1s}e_0,\ \boldsymbol{\alpha}_2=\boldsymbol{F}^*_2\boldsymbol{f}_1-\boldsymbol{F}^*_{1s}\boldsymbol{e}_1+\boldsymbol{F}^*_{1s,\boldsymbol{X}}+\boldsymbol{F}^*_{2,\boldsymbol{X}}f_0-\boldsymbol{F}^*_{1s,\boldsymbol{X}}e_0,$$

$$\boldsymbol{\alpha}_3=\boldsymbol{F}^*_2f_2-\boldsymbol{F}^*_{1s}e_2+\boldsymbol{F}^*_{1s,\mu}+\boldsymbol{F}^*_{2,\mu}f_0-\boldsymbol{F}^*_{1s,\mu}e_0,$$

$$\boldsymbol{\alpha}_4=\boldsymbol{F}^*_2f_3-\boldsymbol{F}^*_{1s}e_3+\boldsymbol{F}^*_{2,\boldsymbol{X}}\boldsymbol{F}^*_{1s}f_0-\boldsymbol{F}^*_{1s,\boldsymbol{X}}\boldsymbol{F}^*_{1s}e_0-\boldsymbol{F}^*_{1s,\boldsymbol{X}}\boldsymbol{F}^*_2f_0e_0+\frac{1}{2}\boldsymbol{F}^*_{1s,\boldsymbol{X}}\boldsymbol{F}^*_{1s}+\frac{1}{2}\boldsymbol{F}^*_{2,\boldsymbol{X}}\boldsymbol{F}^*_2f_0^2+\frac{1}{2}\boldsymbol{F}^*_{1s,\boldsymbol{X}}\boldsymbol{F}^*_{1s}e_0^2,$$

$$f'_0=-\frac{2v^*_{2\mathrm{d},\boldsymbol{X}}\boldsymbol{F}^*_{1x}}{a^*_{2\mathrm{d}}},\ \boldsymbol{f}'_1=-\frac{2v^*_{2\mathrm{d},\boldsymbol{X}}\boldsymbol{F}^*_{1x,\boldsymbol{X}}}{a^*_{2\mathrm{d}}},\ f'_2=-\frac{2v^*_{2\mathrm{d},\boldsymbol{X}}\boldsymbol{F}^*_{1x,\mu}}{a^*_{2\mathrm{d}}},\ f'_3=-\frac{v^*_{2\mathrm{d},\boldsymbol{X}}\boldsymbol{F}^*_{1x,\boldsymbol{X}}\boldsymbol{F}^*_{1x}}{a^*_{2\mathrm{d}}},$$

$$e'_0=\frac{v_{2\mathrm{c},\boldsymbol{X}}(\boldsymbol{F}^*_{1x}+\boldsymbol{F}^*_3f'_0)}{a^*_{2\mathrm{c}}},\ \boldsymbol{e}'_1=\frac{v_{2\mathrm{c},\boldsymbol{X}}(\boldsymbol{F}^*_3\boldsymbol{f}'_1+\boldsymbol{F}^*_{1x,\boldsymbol{X}}+\boldsymbol{F}^*_{3,\boldsymbol{X}}f'_0-\boldsymbol{F}^*_{1x,\boldsymbol{X}}e'_0)}{a^*_{2\mathrm{c}}},$$

$$e'_2=\frac{v_{2\mathrm{c},\boldsymbol{X}}(\boldsymbol{F}^*_3f'_2+\boldsymbol{F}^*_{1x,\mu}+\boldsymbol{F}^*_{3,\mu}f'_0-\boldsymbol{F}^*_{1x,\mu}e'_0)}{a^*_{2\mathrm{c}}},$$

$$e'_3=\frac{v_{2\mathrm{c},\boldsymbol{X}}}{2a^*_{2\mathrm{c}}}(-2\boldsymbol{F}^*_{1x,\boldsymbol{X}}\boldsymbol{F}^*_3f'_0e'_0+\boldsymbol{F}^*_{3,\boldsymbol{X}}\boldsymbol{F}^*_3f'^2_0-2\boldsymbol{F}^*_{1x,\boldsymbol{X}}\boldsymbol{F}^*_{1x}e'_0+2\boldsymbol{F}^*_{3,\boldsymbol{X}}\boldsymbol{F}^*_{1x}f'_0+\boldsymbol{F}^*_{1x,\boldsymbol{X}}\boldsymbol{F}^*_{1x}e'^2_0+\boldsymbol{F}^*_{1x,\boldsymbol{X}}\boldsymbol{F}^*_{1x}+2\boldsymbol{F}^*_3f'_3),$$

$$\boldsymbol{\beta}_1=\boldsymbol{F}^*_{1x}+\boldsymbol{F}^*_3f'_0-\boldsymbol{F}^*_{1x}e'_0,$$

$$\boldsymbol{\beta}_2=\boldsymbol{F}^*_3\boldsymbol{f}'_1-\boldsymbol{F}^*_{1x}\boldsymbol{e}'_1+\boldsymbol{F}^*_{1x,\boldsymbol{X}}+\boldsymbol{F}^*_{3,\boldsymbol{X}}f'_0-\boldsymbol{F}^*_{1x,\boldsymbol{X}}e'_0,$$

$$\boldsymbol{\beta}_3=\boldsymbol{F}^*_3f'_2-\boldsymbol{F}^*_{1x}e'_2+\boldsymbol{F}^*_{1x,\mu}+\boldsymbol{F}^*_{3,\mu}f'_0-\boldsymbol{F}^*_{1x,\mu}e'_0,$$

$$\boldsymbol{\beta}_4=\boldsymbol{F}^*_3f'_3-\boldsymbol{F}^*_{1x}e'_3+\boldsymbol{F}^*_{3,\boldsymbol{X}}\boldsymbol{F}^*_{1x}f'_0-\boldsymbol{F}^*_{1x,\boldsymbol{X}}\boldsymbol{F}^*_{1x}e'_0-\boldsymbol{F}^*_{1x,\boldsymbol{X}}\boldsymbol{F}^*_3f'_0e'_0+\frac{1}{2}\boldsymbol{F}_{1x,\boldsymbol{X}}{}^*\boldsymbol{F}^*_{1x}+\frac{1}{2}\boldsymbol{F}^*_{3,\boldsymbol{X}}\boldsymbol{F}^*_3f'^2_0+\frac{1}{2}\boldsymbol{F}^*_{1x,\boldsymbol{X}}\boldsymbol{F}^*_{1x}e'^2_0.$$

参考文献(References):

[1] NORDMARK A B. Non-periodic motion caused by grazing incidence in an impact oscillator[J]. *Journal of Sound and Vibration*, 1991, **145**(2): 279-297.

[2] CHIN W, OTT E, NUSEE H E, et al. Grazing bifurcations in impact oscillators[J]. *Physical Review E*, 1994, **50**(6): 4427-4444.

[3] LAMBA H, BUDD C J. Scaling of Lyapunov exponents at nonsmooth bifurcations[J]. *Physical Review E*, 1994, **50**(1): 84-90.

[4] FREDRIKSSON M H, NORDMARK A B. Bifurcations caused by grazing incidence in many degrees of freedom impact oscillators[J]. *Proceedings of the Royal Society of London, Series A: Mathematical, Physical and Engineering Sciences*, 1997, **453**(1961): 1261-1276.

[5] LI Q H, WEI L M, AN J Y, et al. Double grazing periodic motions and bifurcations in a vibro-impact system with bilateral stops[J]. *Abstract and Applied Analysis*, 2014, **2014**: 642589.

[6] XU J Q, CHEN P, LI Q H. Theoretical analysis of co-dimension-two grazing bifurcations in *n*-degree-of-freedom impact oscillator with symmetrical constrains[J]. *Nonlinear Dynamics*, 2015, **82**: 1641-1657.

[7] WEGER J D, WILLEM V D W, MOLENAAR J. Grazing impact oscillations[J]. *Physical Review E*, 2000, **62**(2): 2030.

[8] MOLENAAR J, WEGER J D, WILLEM V D W. Mappings of grazing-impact oscillators[J]. *Nonlinearity*, 2001, **14**(2): 301-321.

[9] ZHAO X P. Discontinuity mapping for near-grazing dynamics in vibro-impact oscillators[J]. *Vibro-Impact Dynamics of Ocean Systems and Related Problems*, 2009, **44**: 275-285.

[10] YIN S, WEN G L, XU H D, et al. Higher order zero time discontinuity mapping for analysis of degenerate grazing bifurcations of impacting oscillators[J]. *Journal of Sound and Vibration*, 2018, **437**: 209-222.

[11] CZOLCZYNSKI K, OKOLEWSKI A, BLAZEJCZK-OKOLEWSKA B. Lyapunov exponents in discrete modelling of a cantilever beam impacting on a moving base[J]. *International Journal of Non-Linear Mechanics*, 2017, **88**: 74-84.

[12] BLAZEJCZK-OKOLEWSKA B, CZOLCZYNSKI K, KAPITANIAK T. Dynamics of a two-degree-of-freedom cantilever beam with impacts[J]. *Chaos, Solitons and Fractals*, 2009, **40**(4): 1991-2006.